

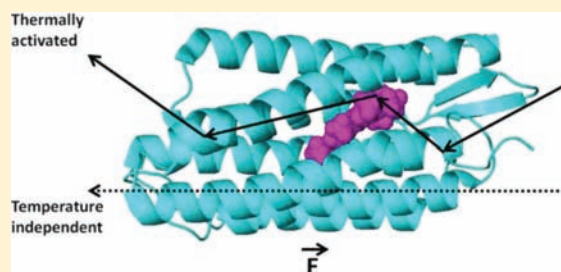
Temperature-Dependent Solid-State Electron Transport through Bacteriorhodopsin: Experimental Evidence for Multiple Transport Paths through Proteins

Lior Sepunaru,^{†,‡} Noga Friedman,[‡] Israel Pecht,[§] Mordechai Sheves,^{*,‡} and David Cahen^{*,†}

[†]Departments of Materials and Interfaces, [‡]Organic Chemistry, and [§]Immunology, Weizmann Institute of Science, POB 26, Rehovot 76100, Israel

Supporting Information

ABSTRACT: Electron transport (ETp) across bacteriorhodopsin (bR), a natural proton pump protein, in the solid state (dry) monolayer configuration, was studied as a function of temperature. Transport changes from thermally activated at $T > 200$ K to temperature independent at <130 K, similar to what we have observed earlier for BSA and apo-azurin. The relatively large activation energy and high temperature stability leads to conditions where bR transports remarkably high current densities above room temperature. Severing the chemical bond between the protein and the retinal polyene only slightly affected the main electron transport via bR. Another thermally activated transport path opens upon retinal oxime production, instead of or in addition to the natural retinal. Transport through either or both of these paths occurs on a background of a general temperature-independent transport. These results lead us to propose a generalized mechanism for ETp across proteins, in which tunneling and hopping coexist and dominate in different temperature regimes.



INTRODUCTION

Over the past decade we have developed experimental methods for fabricating electrically stable solid-state electronic junctions of proteins between two electrodes.¹ The proteins are prepared in a “dry” configuration, where the macroscopic electrodes are non-invasive and non destructive to the protein. (Only the tightly bound structural water is retained. Also it is likely that in all experiments there is no water monolayer on the protein surface, but this requires further study). Consequently, we can measure the resultant currents via these junctions with high reproducibility over the applied bias range of ± 1 V. The currents’ amplitudes measured as a function of bias across a given protein-based junction with a defined area and sufficient surface coverage allow deriving the conduction properties of the examined protein. An advantage of studying electron transport (ETp) in the solid state compared with studies of electron transfer, ET, in solution, is that the system is confined in its dimensions between the electrodes. Therefore, the contribution of the tunneling matrix element H_{AB} (cf. expression for ET in the Marcus ET theory²) to the transport is constant. [H_{AB} may be influenced by the floppiness (low-lying vibrational states) of the system, which in turn can be affected by temperature.^{9,10} However, because our measurements are not time-dependent, stochastic fast fluctuations are probably averaged out (see discussion).] In other words, the distance separating the donor and acceptor analogues (i.e., the electrodes) in this system is fixed. This is different from electrochemical measurements of the rate of electron transfer

(k_{ET}), which is often measured as a function of “ l ” – the distance separating donor and acceptor.³

Therefore, to study ETp in a solid state configuration, we turned to the measurement of current in response to applied bias as a function of temperature, using a well-defined monolayer that contains the protein bacteriorhodopsin, bR.

The bR that is found in *Halobacterium salinarum* consists of seven transmembrane α -helices. Central to its function as a proton pump is the covalent bond between its retinal chromophore and the Lys 216 residue through a protonated Schiff base, $\text{Lys}-\text{N}(\text{H})^+=\text{C}(\text{H})\text{R}$.⁴ bR can maintain functionality even under acute stresses such as wide pH range and high temperatures and, as judged by examining its photocycle, in the solid state (where only the tightly bound water is retained) as well.⁵ These characteristics led to interest in bR as an active component in bioelectronics. Thus, bR (and other proteins as well) have been used as part of a photovoltaic cell,^{6a,b} as the active part of an image sensor,⁷ or as an optical information recording element.⁸ However, in most cases, understanding of electronic charge transport mechanisms within and across proteins is absent or limited.

The ability to macroscopically measure properties of an assembly, containing a large number of molecules, i.e., measure the behavior of many molecules simultaneously, yields relatively large currents, i.e., signals with high Signal to Noise ratio and with good reproducibility (error of 10%). This is important as

Received: October 16, 2011

Published: February 1, 2012

we do not have a clear picture of the voltage profile across the junction. However, our results (below) clearly show that bR is a significant part of the junction and, thus, the voltage drop across the protein must be significant. As shown here, the data indeed provide significant insight into the mechanisms of ETp across bR.

RESULTS AND DISCUSSION

Solid-state ETp measurements have been carried out over a wide temperature range (between 40 and 400 K), without modifying the system, as is the case for solution measurements (for example, adding glycerol to the solvent water so as to enable use of lower temperatures). Because the measured current magnitude expresses the rate of electron transport, we can generalize the resultant current, I , as follows:^{11,12}

$$I \propto k_{\text{ET}} = k_{\text{TI}} + k_{\text{TA}} \quad (1)$$

where k_{TI} and k_{TA} are the electron transfer rates of a temperature-independent and a thermally activated process, respectively. If the two processes occur in parallel, the total current can be expressed as follows:¹³

$$I = A \exp(-\beta I) + B \exp(-E_{\text{A}}/kT) \quad (2)$$

where β is the distance-decay constant, E_{A} is the activation energy of ETp, and k_{B} and T are the Boltzmann constant and the system's absolute temperature, respectively. If sufficiently high temperatures can be reached, the second term will dominate ETp, leading to a general Arrhenius-type relation between current and temperature.

Wild Type Bacteriorhodopsin Junction. Experiments were carried out using the junction preparation procedure detailed in the Experimental Section. In brief, an oxide layer of controllable thickness (~ 1 nm) was grown on a p^{2+} Si wafer. Then, a monolayer of (3-aminopropyl)trimethoxysilane (APTMS) linker was immobilized on the surface to enable electrostatic immobilization of the bR protein on top of the linker. Figure 1 shows the temperature dependence of the current density across a junction, consisting of a monolayer of native, wild type (WT) bR, reconstituted in an OTG matrix under +50 mV bias applied to the top electrode. The current density (J) (current per cm^2 area) was calculated from the currents, measured across a contact area, defined by a circular 500 μm diameter Au pad. Currents were measured at +50 mV bias so as to keep the system as close as possible to equilibrium; at low bias, the current–voltage behavior of the junction is approximately ohmic. The results, shown in Figure 1a, can be divided into four main temperature regimes. At temperatures below 130 K the current is practically temperature-independent ($E_{\text{A}} < 5$ meV). Over the $130 < T < 170$ K temperature range, a decrease in current was observed upon increasing temperature. Raising the temperature above 170 K led to thermally activated transport, which becomes exponentially dependent on temperature above 200 K. Last, between temperatures of 350 and 360 K, a strong increase in current occurs, larger than over the lower temperature range. The employed junctions produced the same results regardless of whether the sample's temperature was increased or decreased; in other words, the results were reproducible and reversible over the whole temperature range (see Supporting Information, Figure S1). In addition, junctions with an APTMS linker layer only (see Experimental Procedure and Setup section) showed (orders of magnitude higher) temperature independent currents over the whole temperature range (Figure S2, Supporting Information).

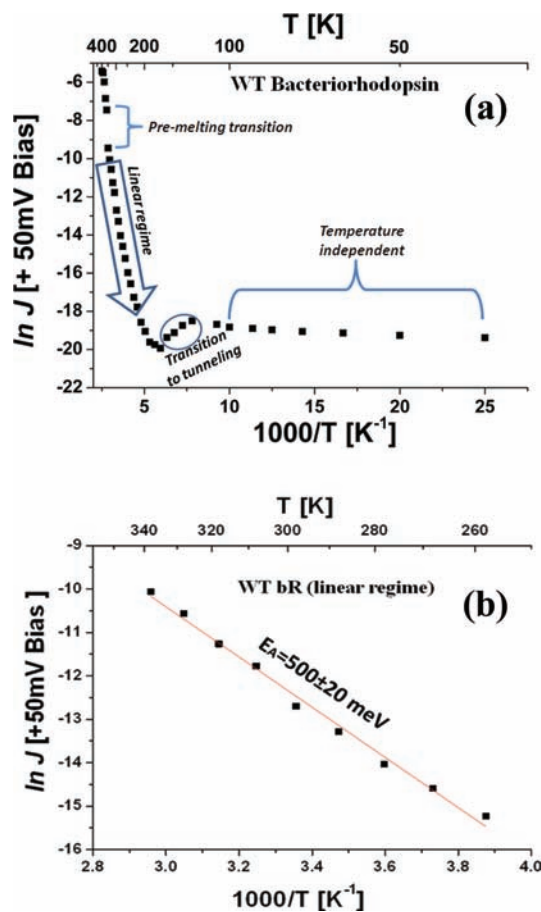


Figure 1. (a) $\ln(\text{current density})$ –temperature dependence via WT bR monolayer junctions at +50 mV bias to the top electrode. (b) Arrhenius plot, for higher temperature data, yielding the calculated activation energy of 500 meV.

The only report of temperature dependent electron transport across bR was in a transistor configuration.¹⁴ That study, aimed at investigating Coulomb blockade effects in a single bR fragment, indicated a 47 meV thermal activation energy over a 4–174 K temperature range (extracted from zero bias conductance), higher than the upper limit that we estimate for our system between 130 and 40 K. More temperature-dependent ETp results were reported for monolayer or single molecule samples of organic molecules,¹⁵ polymers,^{16,17} peptides,^{18,19} and DNA in a solid state configuration.^{20,21} The results presented here indicate thermally activated ETp across a well-defined WT bR monolayer at temperatures from 200 K upward.

The lack of temperature dependence of the currents at $T < 130$ K is rather surprising, because temperature independent transport is normally associated with coherent tunneling. The occurrence of such a process across a >5 nm junction (cf. a value based on the known 3D structure of bR,²² as well as our own AFM results⁵) is unexpected. From recent studies comparing conjugated molecules of varying length, it was concluded that there is a transition from a tunneling to a hopping (thermally activated) mechanism across a molecular separation of ~ 5 nm.^{15,23} Thus, taking into account the observed low currents in this regime, tunneling, even if it has a low probability, cannot be ruled out.

In view of these results, we attribute the decrease of current with increasing temperature between $130 < T < 170$ K to a

transition from a temperature independent to a thermally activated ETp mechanism. As the temperature over this range decreases, the efficiency of thermally activated hopping transport becomes lower than that via the alternative tunneling path. This transition can be explained by a change in the protein to a more rigid conformation as the thermal energy decreases. While tunneling is, to a first approximation, temperature independent, currents across 1–2 nm long nonconjugated alkyl chains showed, down to $T = 120$ K, an inverse metallic-like (negative) temperature dependence; that is, currents increased with decreasing temperature.²⁴ This is explained in part by the decrease in defects with decreasing temperature. Assuming a similar tunneling behavior here, we can rationalize the observed increasing current with decreasing temperature in the 170–130 K temperature range by a transition to a less defective structure of the monolayer.

Figure 1a and the zoom-in on high temperatures between $260 < T < 340$ K in Figure 1b show that at physiological temperatures ETp via WT bR is thermally activated. At high temperatures ($T > 200$ K), $\ln(J)$ is found to be inversely proportional to temperature (Figure 1b), and any contribution from a temperature independent mechanism is negligible. In other words, the second term in eq 2 dominates, and a 500 ± 20 meV activation energy for ETp is calculated from the data.

Our previous studies of azurin and bovine serum albumin showed that temperature dependent currents are sensitive to the protein's native structure.²⁵ Hence, it is reasonable to assume structural changes of bR as the cause of the transition seen in Figure 1a. The jump to higher currents around 350–360 K fits well with results of studies on the structural stability of bR. bR undergoes a reversible premelting conformational transition at these temperatures,^{26,27} and indeed, we find the 350–360 K transition to be fully reversible. The stability of bR at high temperatures and the significant 0.5 eV activation energy yielded current densities at ~ 400 K that exceed mA/cm^2 at a bias of 50 mV; that is, bacteriorhodopsin is definitely not an insulator!²⁸

To shed further light on the origin of the currents' stability at high temperatures, we have also conducted a set of experiments at higher relative humidity, rather than the low vacuum, low humidity conditions employed in all other measurements described here (see Experimental Procedure and Setup). This required a change in the experimental setup to one that is used regularly²⁹ where a hanging Hg top contact is employed, and the addition of a heating plate. At low relative humidity (RH) of 20%, the activation energy calculated from the temperature dependence measurements was similar to that observed in low vacuum in the range 290–370 K (see Supporting Information, Figure S3). However, as indicated in Figure 2, at RH = 85%, the activation energy increased to ~ 1 eV. In addition, a sharp irreversible decrease in current was observed at 360 K, which we ascribe to protein denaturation, in keeping with the reported denaturation temperature of bacteriorhodopsin in water suspension.³⁰ These results highlight the crucial role that bR's tertiary structure plays in ETp. We attribute the increase in activation energy (E_A) to a higher barrier, possibly caused at higher RH by a water layer formed on top of the sample. This explanation is consistent with the finding that bR contains a water layer on its surface at RH higher than ca. 60%.³¹

Another important observation, emerging from the temperature dependence studies is that, at lower RH, high temperatures do not cause the sharp decrease in the current, which we interpret to show that under these conditions WT bR is not

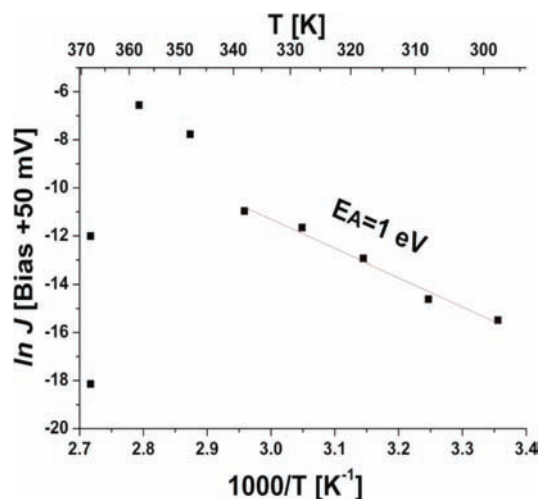


Figure 2. Temperature dependence of $\ln(\text{current density})$ across the WT bR monolayer junction with Hg as top electrode at +50 mV bias to the top electrode in RH = 85%. An irreversible decrease in current occurs at $T \sim 368$ K, which corresponds to denaturation of the protein. There are two points at the same temperature because denaturation takes ~ 15 min to be completed.

denatured up to the highest temperatures at which we can measure. This result agrees with the known³² high thermal stability of bR films in vacuum up to 140°C (413 K), relative to hydrated films. It appears that increased bR thermal stability under relatively dry conditions occurs also in the monolayer and not only, as reported earlier, in multilayer films.

Modified Bacteriorhodopsin Junctions. Results of studies of the temperature and separation length dependence of ET and of ETp (in molecular electronics) generally enable resolving between hopping and tunneling. Additional support for the operation of either mechanism can be derived by introducing a structural change of a specific site in the protein monolayer junction, where the charge might reside transiently (for hopping).³³ In the case of protein-based junctions, mutations or chemical modifications can be introduced, and the latter approach has been taken here in order to examine the role of retinal as a possible electron resident site.

A. Apo bR and Reduced bR. To examine the role of the retinal moiety in ETp across bR, samples of bR were prepared in a way in which the retinal–protein linkage was modified as follows:

- (1) Reduced bR: The retinal–protein protonated Schiff base double bond was reduced to yield a C–N single bond ($\text{Lys}-\text{N}(\text{H})^+=\text{C}(\text{H})-\text{R} \rightarrow \text{Lys}-\text{N}(\text{H})-(\text{H})\text{C}(\text{H})-\text{R}$), thus eliminating the chromophore's positive charge.
- (2) Apo bR: bR treatment with hydroxyl amine eliminates the retinal–protein covalent bond, and the retinal is converted to a noncovalently bound retinal oxime ($\text{Lys}-\text{N}(\text{H})^+=\text{C}(\text{H})-\text{R} \rightarrow \text{Lys}/\text{HO}-\text{N}=\text{C}(\text{H})-\text{R}$). It was suggested that a fraction of the formed retinal oxime resides in the native retinal binding site while another fraction is partially distributed in another, as yet unknown, region of the membrane–protein complex.^{34,35}

As can be seen from Figure 3, currents via junctions with reduced bR (triangles) exhibited temperature dependence, similar to that of WT bR. In contrast, eliminating the retinal–

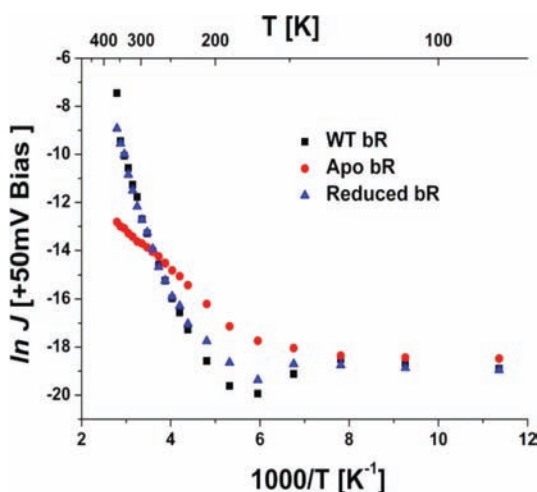


Figure 3. $\ln(\text{current density})$ –temperature dependence via junctions with modified bR monolayer forms at +50 mV bias to the top electrode.

protein covalent bond (Apo bR, circles) considerably changed the ETp temperature dependence. The activation energy calculated for ETp across apo bR was 180 ± 20 meV, much lower than that for WT bR. The result with reduced bR implies that the nitrogen positive charge and type of retinal linkage to the protein do not significantly affect the ETp process. The result with apo bR indicates that removal of the retinal–protein covalent bond and/or the formation of retinal oxime and/or its removal from the binding site leads either to a new ETp pathway or to a lower ETp barrier for the part that is operative in WT bR.

B. Reconstituted bR (from apo bR) and WT bR, Incubated with Retinal Oxime. To resolve the origin of the behavior of apo bR, we reconstituted bR by incubating apo bR with retinal. The reconstituted protein is known to contain both a covalently bound retinal and retinal oxime.^{34,35} To examine if retinal oxime plays a specific role, we prepared samples of WT bR to which an equivalent amount of retinal oxime was added, leading to a product, similar to that of reconstituted bR (from apo bR). The results (Figure 4a triangles, green circles) show very similar behavior and activation energies for both these products.

Figure 4a clearly indicates that the $\ln(\text{current density})$ as a function of $1000/T$ plot at +50 mV bias yields two different activation energies for the junction made with bR, reconstituted from apo bR (green circles) with an inflection around 260 K. The activation energies calculated from the linear regime are 180 and 490 meV (Figure 4b), matching those of apo bR and of WT bR, respectively.

It is possible to describe these observations in terms of two distinct processes having different activation energies, namely:

$$I = A \exp\left(\frac{-E_{A,\text{retinal}}}{k_B T}\right); \quad T > 260 \text{ K}$$

$$I = A \exp\left(\frac{-E_{A,\text{retinal oxime}}}{k_B T}\right); \quad 200 < T < 260 \text{ K} \quad (3)$$

Over the low temperature regime, the “jump” in the currents, observed around $130 < T < 170$ K in WT bR, is absent in apo bR and in bR, reconstituted from apo bR. In other words, in bR, reconstituted from apo bR, ETp can occur via two

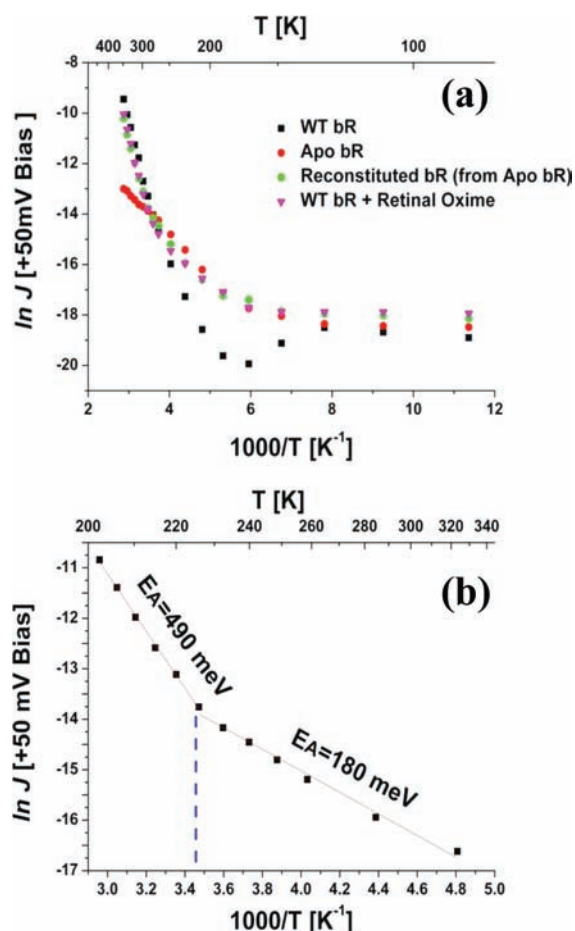


Figure 4. (a) Temperature dependence of $\ln(\text{current density})$ via junctions with modified bR monolayer forms at +50 mV bias to the top electrode. (b) Arrhenius plot, for higher temperature of reconstituted bR (from apo bR), produced two calculated activation energies from the $\ln(I)$ – T plot. A transition from low to high activation energy is observed around $T = 260$ K. This change may indicate a change from one ETp pathway via the retinal oxime at low temperature to another ETp pathway, involving retinal.

pathways, one with a high thermal activation energy, as in WT bR, and one with a lower activation energy at temperatures < 260 K, as in apo bR. From this behavior we deduce that ETp follows Kirchhoff’s law, where the electrons flow via the most conductive thoroughfare. In addition, the sensitivity to retinal oxime modification suggests the importance of the presence of retinal, rather than to its covalent binding to the protein’s epsilon lysine residue. Both results (reconstituted bR from apo bR and WT bR + retinal oxime) support the idea that relocation of the retinal (as retinal oxime) to a different region in the protein opens a new pathway for ETp, in addition to that provided by the retinal in its natural binding site.

C. Washed apo bR, Washed Reconstituted bR, and Amino Acids Contribution. To further resolve the contribution of the retinal moiety to ETp, retinal oxime was completely removed from apo-membrane (washed apo bR). Arrhenius plots shown in Figure 5, (circles) indicate a calculated ETp activation energy of 410 ± 25 meV.

As can be seen from Figure 5b, the currents across washed apo bR junctions (circles) are lower by more than 1 order of magnitude than those across WT bR junctions (150 nA/cm^2 for washed apo bR and $3 \mu\text{A/cm}^2$ for WT bR at 293 K). The 90

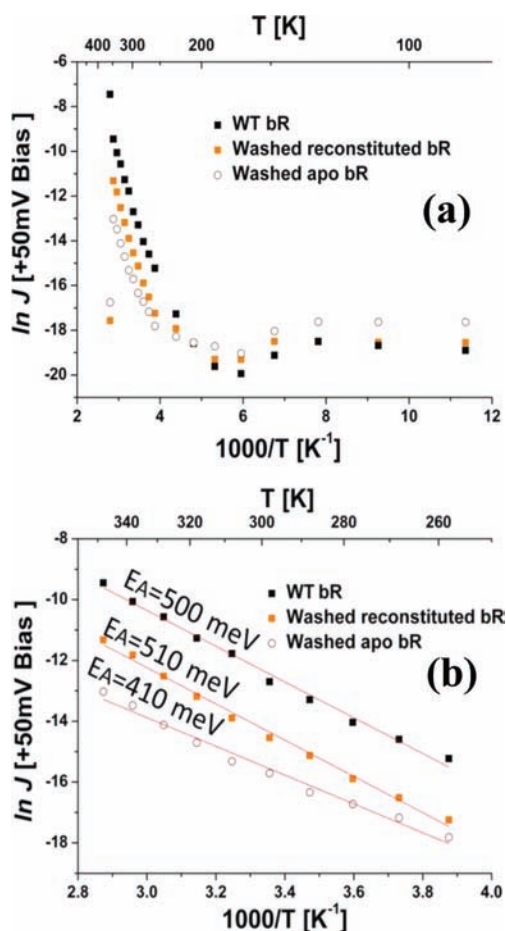


Figure 5. (a) $\ln(\text{current density})$ –temperature plots for junctions with modified bR monolayer forms at +50 mV bias to the top electrode. (b) Arrhenius plots for the currents at higher temperatures across (modified) bR and calculated activation energies.

meV decrease in activation energies for the proteins without retinal could suggest that the ETp mechanism is indeed dependent on the presence of retinal. However, in view of the severe chemical treatments that were required to prepare the washed apo bR samples prior to immobilization, we cannot exclude the possibility that the decrease in the total current magnitude is due in part or fully to a treatment-induced change in the protein or in its bound lipids.

To try and resolve between these possibilities, we carried out an additional set of experiments, using reconstituted bR in which retinal oxime and excess retinal were removed from the protein (washed reconstituted bR). We find that the shape of the temperature dependence of ETp across retinal oxime free reconstituted bR (Figure 5a,b (orange squares)) and the activation energy are both similar to those of WT bR, while the current amplitudes are intermediate between those of WT bR and washed apo bR (500 nA/cm² at 293 K). Therefore, we conclude that the observed decrease in currents via the washed samples is in part a result of the rather harsh washing conditions prior to immobilization. This explanation is reinforced by the appearance of an irreversible sharp decrease of the currents for the junctions with the washed samples at high temperatures, probably due to denaturation, suggesting the formation of a protein that is less stable than that of WT bR at high temperature. It is plausible that the employed hexane treatment also removes part of the associated lipids, which leads

to a loose packing of the protein–membrane complex. This observation can be attributed to a decrease in the pre-exponential factor of the current expression in eq 2. A possible cause for this is that the electronic coupling to the electrodes has been lowered due to these modifications.

Washed apo bR samples show a decrease not only in the currents but also in the activation energy. As noted above, though, the activation energy of ETp across the washed reconstituted bR sample is similar to that for the WT bR samples (within the experimental error range). Therefore, comparing the results obtained with these three types of samples, we suggest that the decrease in currents and activation energies is a direct result of elimination of the covalent bond between the retinal and the protein. However, we cannot exclude the possibility that this bond breakage also affects the protein's conformation, which causes the above changes.

Taken together, the above results lead us to the conclusion that there should be additional protein elements that contribute to the thermally activated transport, for example that of specific amino acids. This conclusion is further reinforced by comparing the temperature dependence of the current through proteins having a prosthetic group and those that do not. Figure 6

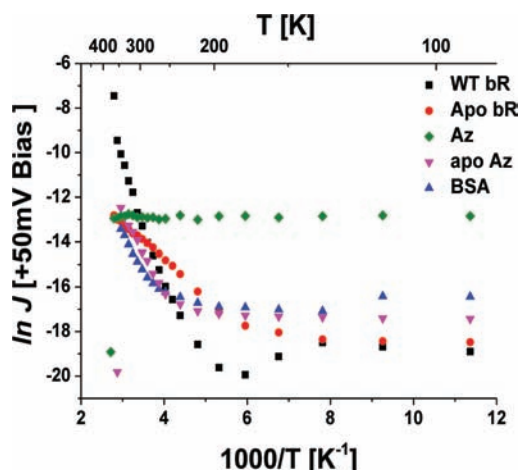


Figure 6. $\ln(\text{current density})$ –temperature plots of junctions with (modified)bR, (modified)azurin, and bovine serum albumin monolayers, at +50 mV bias to the top electrode. Except for azurin, all the examined proteins behave similarly, with thermally activated ETp dominating at temperatures >200 K and virtually temperature-independent behavior below ~ 120 K.

demonstrates that the transition from temperature-independent to thermally activated ETp is observed for all proteins that we examined so far, except for holo azurin.²⁵ The different temperatures at which thermally activated ETp is observed might evolve from the different conditions under which the thermal protein fluctuations enable the activated ETp. In the case of azurin, it is the copper ion, which enables the coherent tunneling (or two-step coherent tunneling³⁶) over the whole temperature regime up to its denaturation. Possibly, if Az were stable until higher temperatures, incoherent hopping would start to dominate, as in all other cases.

CONCLUSIONS

Temperature-dependent current via WT bR and its different derivatives shows that both temperature-independent and dependent pathways can coexist. It is unlikely that the

electrode/protein contact barriers are the cause for the temperature dependence as

- both types are observed in the same sample (but each one dominates over a different temperature range); and
- all measured temperature dependences remain unchanged under applied voltages of up to 1 V (see Figure S4, Supporting Information), the maximal applied bias between electrodes in this study.

The power of the present approach lies in the sensitivity of the measuring system to the ET_p mechanism, which, in turn, depends on structural changes in the protein as well. Our results indicate that the retinal chromophore is involved in the strong thermally activated ET_p across a WT bR monolayer. This pathway remains active up to above 400 K (the maximum temperature that can be reached with the used measuring system) and allows high current densities (>mA/cm²) across WT bR, already at a low bias of 50 mV. Such current densities at very low bias are inconsistent with the view that proteins are electronic insulators. Thus, electronic signals via a protein based junction might become feasible for, for example, sensing applications.

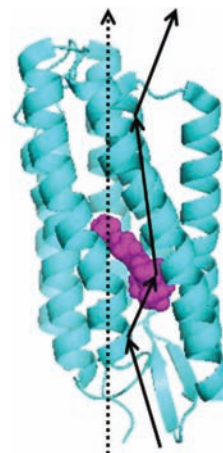
Retinal oxime adsorbed by the apo bR acts as electron mediator with lower activation energy than that of the retinal, which is covalently bound to its binding site. This lower activation energy makes the retinal oxime pathway the dominant one below 260 K in reconstituted bR, where both retinal oxime and bound retinal are present. The observation of different current magnitudes at a given temperature for different bR variants allows comparison between them. For example, at 200 K, currents of 8.5, 90, and 60 nA/cm² are observed for WT bR, apo bR, and reconstituted bR (from apo bR), respectively (Figure 4a). Therefore, we conclude that a distinct ET_p pathway is formed in apo bR that has not been caused by eliminating the retinal–protein covalent bond, but rather by the presence of retinal oxime.

Reconstitution of bR (from apo bR) produces a two-state system (with two pathways), each of which dominates over a different temperature range, because current passes through the path of the least resistance. At low temperatures ($T < 130$ K) tunneling is most efficient, while at higher temperature current flows via a thermally activated process involving the retinal oxime. At $T > 260$ K, the pathway via retinal has the lowest resistance; hence, it is the most efficient one. This switch is a result of the higher activation energy via the retinal pathway. While dual ET_p pathways exist naturally in proteins, e.g., in the photosystem I reaction center,³⁷ we are not aware of observations of dual ET_p pathways caused by protein modification as in this case.

The results of this report show similarity to observations in optical spectroscopy ET measurements through the photosynthetic bacterium *Chromatium*.³⁸ In that study, a transition from coherent quantum mechanical tunneling to thermally activated electron transfer was observed. The probability for tunneling remains constant until vibrational states are excited, allowing access to an activated process (which, for *Chromatium*, occurs at $T > 100$ K). Recent neutron scattering of bR^{39,40} and myoglobin⁴¹ and theoretical work as well⁴² indicate a transition to a “glassy” state in these proteins upon cooling below 200 K. In this glassy state, there is a constant temperature-independent low mean square displacement of the atoms inside the protein. In other words, below 200 K, the proteins act more as a rigid, “lattice-like” material than as a fluctuating system.

On the basis of the results of the above studies and of ours on bR, azurin, and BSA, we propose a schematic picture for electron transport across proteins. In Scheme 1, we present a

Scheme 1. Proposed Model for a General Electron Transport Process across Proteins^a



^aThe scheme shows a single bR protein; pdb file 1R2N, cartoon presentation + retinal in sphere), showing tunneling and hopping mechanisms, operating in parallel. At low temperatures, tunneling dominates, while, at higher temperatures (>200 K), the tunneling currents, which are temperature-independent, remain low and hopping becomes the more efficient ET_p path. For reconstituted bR (from apo bR), we interpret our data in terms of three different pathways: two thermally activated ones, one at $T > 260$ K and one at $200 < T < 260$ K (only one of which is shown), together with tunneling ET_p that dominates at low temperatures.

3D structure of a single bacteriorhodopsin unit and the proposed simplified electron transport mechanisms. Our suggestion is that tunneling and hopping mechanisms operate in parallel (see Scheme 1, dotted line = tunneling, line = hopping). At low temperatures, $T < 200$ K, thermally activated hopping currents become negligible, and (low) tunneling currents are detected. At higher ($T > 200$ K) temperatures, those low currents (low tunneling probability) are masked completely by the currents originated from the hopping mechanism.

This picture may be relevant to electron transport as well as to electron transfer. Differences between the employed experimental conditions (solution vs dry) may dictate the flexibility of the system (fluctuations, vibrations, etc), which is important for tunneling to be dominant, but will not change the general behavior. We stress that the shorter the distance over which electron transfer is measured, the higher the probability for tunneling. This is important, because, for a given protein, the distance over which ET is measured is mostly less than that for the ET_p measurement, which is dictated by the electrodes. Consequently, efficient tunneling can mask any thermally activated mechanism over the temperature range that is accessible in ET studies.

For bR from which both retinal and retinal oxime have been removed (washed apo bR), we find a thermal activation energy of ~ 410 meV, suggesting that also the polypeptide matrix of the protein provides a thermally activated ET_p pathway. Such a process may be hopping via individual amino acids residues.⁴³ The latter process is currently studied in our laboratory by measuring ET_p across different oligopeptides.

In our experiments all the measured currents at a specific voltage are averaged and the integration time is ~ 30 ms. Time-dependent current–voltage measurements as a function of temperature that are underway may help to improve on and refine the present schematic picture.

EXPERIMENTAL PROCEDURE AND SETUP

The sampling method, which has been employed here, is a standard $I-V(T)$ measurement. The materials that were used are detailed fully elsewhere.¹ In brief, a heavily doped (highly conducting) p-Si wafer ($\rho < 0.0009$ [$\Omega\cdot\text{m}$]) was cut into small pieces of $1\text{ cm} \times 1\text{ cm}$. The pieces were cleaned by a standard procedure and etched with 2% HF to remove the native oxide. Immediately after the etching, a 10 \AA thick oxide layer was grown controllably, by immersion in piranha solution. The resulting surface was incubated overnight in a solution of (3-aminopropyl)trimethoxysilane (3-APTMS, Aldrich, 10% in methanol) to form an NH_2 terminated, positive headgroup linker to connect the proteins to the surface with minimal additional electrical resistance.

Purple membrane fragments from *Halobacterium salinarum* were purified by a standard method.⁴⁴ Membrane vesicles were prepared following the procedure of Kouyama et al.⁴⁵ Briefly, the native membrane fragments were partially delipidated using tween-20 detergent, followed by incubation with octylthioglucoside (OTG) at $55\text{ }^\circ\text{C}$ for 5 days, leading to formation of bR vesicles. Therefore, all bR forms are with OTG detergent.

Reduced-bR OTG: bR-OTG in phosphate buffer (0.01 M, pH 6.4) and ammonium sulfate (0.1 M) (10^{-5} M, 1 mL) was reduced by illumination in the presence of NaBH_4 (ca. 20 mg). Following completion of the reduction process (3 h), the suspension was dialyzed against a solution of phosphate buffer (0.01 M, pH 6.4) and ammonium sulfate (0.1 M).

Apo-bR OTG: bR-OTG was bleached by illumination in the presence of NH_2OH (2 M, pH 7.2) and dialyzed against a solution of phosphate buffer (0.01 M, pH 6.4) and ammonium sulfate (0.1 M).

Reconstituted bR-OTG: Apo-bR OTG in phosphate buffer (0.01 M, pH 6.4) and ammonium sulfate (0.1 M) (10^{-5} M, 1 mL) was incubated with a retinal dissolved in EtOH (1.2×10^{-3} M, $10\text{ }\mu\text{L}$). The reconstitution process was completed in 30 min.

bR OTG + Retinal Oxime: Retinal oxime solution in EtOH (10^{-3} M, $10\text{ }\mu\text{L}$) was mixed with bR-OTG in phosphate buffer (0.01 M, pH 6.4) and ammonium sulfate (0.1 M) (10^{-5} M, 1 mL). Retinal oxime was obtained by incubating retinal solution in EtOH (10^{-5} M, 1 mL) with hydroxyl amine solution in water (0.1 M, $10\text{ }\mu\text{L}$).

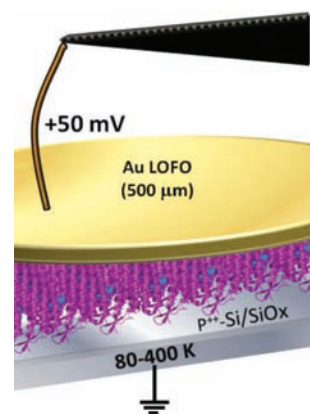
Washed protein: a suspension of apo-OTG or reconstituted bR-OTG (10^{-5} M, 1 mL) was mixed with *n*-hexane (1.3 mL) and was sonicated (sonicator bath, 2 min). The mixture was spun down, and the organic layer was discarded. The same procedure was repeated 3–4 additional times, until no retinal oxime was detected by absorbance measurement.

The APTMS-terminated samples were incubated in a suspension of bR-OTG, or modified bR-OTG (10^{-5} M, 2 mL, 20 min), followed by incubation in a water bath (3 h) where vesicle fusion took place. The substrates were gently rinsed in water and dried under a stream of N_2 . At each stage, the samples were characterized by ellipsometry, AFM, and XPS.

To close the electrical circuit that includes the protein, we used a nondestructive method for top contact deposition. In all cases except for the 85% RH measurements, we used Au pads as top contacts.⁴⁶ In this method Au pads, $500\text{ }\mu\text{m}$, corresponding to an effective contact area of 0.2 mm^2 were evaporated on cleaned glass slides. The Au pads were then Lifted Off and Floated On (LOFO) by immersing the glass slides quickly in 2% HF solution to separate the Au from the glass; the pads were transferred into a large volume of water ($18\text{ M}\Omega$), a liquid on which they float. The protein-covered surfaces were inserted with tweezers beneath the floating pads and lifted so that they were removed from the liquid with the Au pad on top. The full junction was dried under a gentle flow of pure N_2 and transferred into a low vacuum (0.1 mbar) chamber for at least 0.5 h to remove any water between the pads and the proteins. In the case of measurements not in vacuum (see

Figure 2), we used a Hg drop with the same effective contact area as top contact. The junctions with Au and Hg were compared by measuring both under ambient conditions, resulting in similar current densities and $I-V$ curves (see Supporting Information Figure S3).

Scheme 2. Scheme of the Final Junction Configuration with a LOFO Nondestructive Top Contact with an Effective Area of 0.2 mm^2



After formation of the full protein based junction (Scheme 2), the sample was connected via a $17.5\text{ }\mu\text{m}$ thick gold wire to macroscopic probes, connected to an $I-V$ measurement system (Keithley). Prior to connection of the wire to the Au LOFO electrode, a small bias of 10 mV was applied, so that current could be used as a criterion for establishing stable contact. Measurements were initiated only after stable currents were achieved. All our results were obtained on macroscopic areas (0.2 mm^2 contact area, containing 10^9 – 10^{10} protein molecules). The sample was placed in a low vacuum (0.1 mbar) chamber in a TTPX cryogenic system (Lakeshore), and both the sample holder and the probes were cooled. Temperature was monitored and controlled with an accuracy of 0.2 K. Between each change in temperature, the sample was not measured, so as to allow it to reach thermal equilibrium. The deviations from the average observed currents were 10% for all measurements. Therefore, all results reported here correspond to the averaged observed current, with upper and lower limits deviating by up to 10% from the averaged currents. For all measurements, short circuit currents (2 – $3\text{ }\Omega$) were measured before and after the temperature-dependent measurement series to ensure proper connections were maintained during the whole experimental process.

ASSOCIATED CONTENT

Supporting Information

$\ln(\text{current density})$ –temperature dependence upon cooling and heating (reversibility); $\ln(\text{current density})$ –temperature dependence via ATPMS (linker); $I-V$ curves of WT bR junctions at different humidities and with different top contacts; $\ln(\text{current density})$ as a function of applied bias, via WT bR monolayer junctions at different temperatures. This material is available free of charge via the Internet at <http://pubs.acs.org>.

AUTHOR INFORMATION

Corresponding Author

Mudi.Sheves@weizmann.ac.il; David.Cahen@Weizmann.ac.il

Notes

The authors declare no competing financial interest.

■ ACKNOWLEDGMENTS

We thank Israel Bar-Joseph for use of the $I-V-T$ probe station and Hagay Shpaisman for help and advice on use of the system. M.S. holds the Katzir–Makineni chair in chemistry. D.C. holds the Schaefer Chair in Energy Research. We thank the Minerva Foundation (Munich), the Kimmel Centre for Nanoscale Science, and the Kimmelman center for Biomolecular Structure and Assembly for partial support. L.S. thanks the Israeli Ministry of Science and Technology for an Eshkol scholarship.

■ REFERENCES

- (1) Ron, I.; Pecht, I.; Sheves, M.; Cahen, D. *Acc. Chem. Res.* **2010**, *43*, 945–953.
- (2) Marcus, R. A.; Sutin, N. *Biochim. Biophys. Acta* **1985**, *881*, 265–322.
- (3) Langen, R.; Chang, I. J.; Germanas, J. P.; Richards, J. H.; Winkler, J. R.; Gray, H. B. *Science* **1995**, *268*, 1733–1735.
- (4) King, G. I.; Mowery, P. C.; Stoeckenius, W.; Crespi, H. L.; Schoenborn, B. P. *Proc. Natl. Acad. Sci. U.S.A.* **1980**, *77*, 4726–4730.
- (5) Ron, I.; Sepunaru, L.; Itzhakov, L.; Belenkovaet, T.; Friedman, N.; Pecht, I.; Sheves, M.; Cahen, D. *J. Am. Chem. Soc.* **2010**, *132*, 4131–4140.
- (6) (a) Karvaly, B.; Dancsházy, Z. *FEBS Lett.* **1977**, *76*, 36–40.
(b) Carmeli, I.; Frolov, L.; Carmeli, C.; Richter, S. *J. Am. Chem. Soc.* **2007**, *129*, 12352–12353.
- (7) Miyasaka, T.; Koyama, K. *Appl. Opt.* **1993**, *32*, 6371–6379.
- (8) Hampp, N. *Chem. Rev.* **2000**, *100*, 1755–1776.
- (9) Xie, Q.; Archontis, G.; Skourtis, S. S. *Chem. Phys. Lett.* **1999**, *312*, 237–246.
- (10) Balabin, I. A.; Onuchic, J. N. *Science* **2000**, *290*, 114–117.
- (11) Liu, H.; Zhao, Z.; Wang, N.; Yu, C.; Zhao, J. *J. Comput. Chem.* **2011**, *32*, 1687–1693.
- (12) Selzer, Y.; Cabassi, M. A.; Mayer, T. S.; Allara, D. L. *Nanotechnology* **2004**, *15*, S483–S488.
- (13) Segal, D.; Nitzan, A. *Chem. Phys.* **2002**, *281*, 235–256.
- (14) Kim, J.; Lee, S.; Yoo, K.; Jang, D. *Appl. Phys. Lett.* **2009**, *94*, 153301–153303.
- (15) Choi, S. H.; Frisbie, C. D. *J. Am. Chem. Soc.* **2010**, *132*, 16191–16201.
- (16) Blom, P. W. M.; de Jong, M. J. M.; van Munster, M. G. *Phys. Rev. B* **2007**, *55*, 656–659.
- (17) Martin, S. J.; Lupton, J. M.; Samuel, I. D. W.; Walker, A. B. *J. Phys.: Condens. Matter.* **2002**, *14*, 9925–9933.
- (18) Arikuma, Y.; Nakayama, H.; Morita, T.; Kimura, S. *Angew. Chem., Int. Ed.* **2010**, *49*, 1800–1804.
- (19) Sek, S.; Moszynski, R.; Sepiol, A.; Misicka, A.; Bilewicz, R. *J. Electroanal. Chem.* **2003**, *550–551*, 359–364.
- (20) Porath, D.; Bezryadin, A.; de Vries, S.; Dekker, C. *Nature* **2000**, *403*, 635–638.
- (21) Yoo, K.-H.; Ha, D. H.; Lee, J.-O.; Park, J. W.; Kim, J.; Kim, J. J.; Lee, H. Y.; Kawai, T.; Choi, H. Y. *Phys. Rev. Lett.* **2001**, *87*, 198102–198105.
- (22) Luecke, H.; Schobert, B.; Richter, H.; Cartailier, J.; Lanyi, J. K. *J. Mol. Biol.* **1999**, *291*, 899–911.
- (23) Choi, S. H.; et al. *J. Am. Chem. Soc.* **2010**, *132*, 4358–4368.
- (24) Salomon, A.; Shpaisman, H.; Seitz, O.; Boecking, T.; Cahen, D. *J. Phys. Chem. C* **2008**, *112*, 3969–3974.
- (25) Sepunaru, L.; Pecht, I.; Sheves, M.; Cahen, D. *J. Am. Chem. Soc.* **2011**, *133*, 2421–2423.
- (26) Wang, J.; Heyes, C. D.; El-Sayed, M. A. *J. Phys. Chem. B* **2002**, *106*, 723–729.
- (27) Wang, J. *Biophys. J.* **1999**, *76*, 2777–2783.
- (28) Page, C. C.; Moser, C. C.; Dutton, P. L. *Curr. Opin. Chem. Biol.* **2003**, *7*, 551–556.
- (29) Yaffe, O.; Scheres, L.; Puniredd, S. R.; Stein, N.; Biller, A.; Har Lavan, R.; Shpaisman, H.; Zuillhof, H.; Haick, H.; Cahen, D.; Vilan, A. *Nano Lett.* **2009**, *9*, 2390–2394.
- (30) Jackson, M. B.; Sturtevant, J. M. *Biochemistry* **1978**, *17*, 911–915.
- (31) Varo, G.; Eisenstein, L. *Eur. Biophys. J.* **1987**, *14*, 163–168.
- (32) Shen, Y.; Safinya, C. R.; Liang, K. S.; Ruppert, A. F.; Rothschild, K. J. *Nature* **1993**, *366*, 48–50.
- (33) Segal, D.; Nitzan, A.; Davis, W. B.; Wasielewski, M. R.; Ratner, M. A. *J. Phys. Chem. B* **2000**, *104*, 3817–3829.
- (34) Friedman, N.; Ottolenghi, M.; Sheves, M. *Biochemistry* **2003**, *42*, 11281–11288.
- (35) Becher, B.; Cassim, J. *Biophys. J.* **1977**, *19*, 285–297.
- (36) Friis, E. P.; Andersen, J. E. T.; Kharkats, Y. I.; Kuznetsov, A. M.; Nichols, J. R.; Zhang, J.-D.; Ulstrup, J. *Proc. Natl. Acad. Sci.* **1999**, *96*, 1379–1384.
- (37) Guergova-Kuras, M.; Boudreaux, B.; Joliot, A.; Joliot, P.; Redding, K. *Proc. Natl. Acad. Sci.* **2001**, *98*, 4437–4442.
- (38) De Vault, D.; Chance, B. *Biophys. J.* **1966**, *6*, 825–847.
- (39) Ferrand, M.; Dianoux, A. J.; Petry, W.; Zaccai, G. *Proc. Natl. Acad. Sci. U.S.A.* **1993**, *90*, 9668–9672.
- (40) Fitter, J.; Lechner, R. E.; Dencher, N. A. *J. Phys. Chem. B* **1999**, *103*, 8036–8050.
- (41) Doster, W.; Cusack, S.; Petry, W. *Nature* **1999**, *337*, 754–756.
- (42) Vitkup, D.; Ringe, D.; Petsko, G. A.; Karplus, M. *Nat. Struct. Mol. Biol.* **2000**, *7*, 34–38.
- (43) Cordes, M.; Giese, B. *Chem. Soc. Rev.* **2009**, *38*, 892.
- (44) Oesterheld, D.; Stoeckenius, W. *Methods Enzymol.* **1974**, *31*, 667–678.
- (45) Denkov, N. D.; Yoshimura, H.; Kouyama, T.; Walz, J.; Nagayama, K. *Biophys. J.* **1998**, *74*, 1409–1420.
- (46) Vilan, A.; Cahen, D. *Adv. Funct. Mater.* **2002**, *12*, 795.